Electronic Supporting Information (ESI) for

Patterned nanofiber air filters with high optical transparency, robust mechanical strength, and effective $PM_{2.5}$ capture capability

Jinshan Cao, [a] Zhiqiang Cheng, *[a] Lijuan Kang, [a] Meng Lin [b] and Lihao Han*[b]

[a]College of Resources and Environment, Jilin Agricultural University, Changchun 130118, People Republic China. E-mail: cjs4451@126.com

[b]Joint Center for Artificial Photosynthesis (JCAP), California Institute of Technology (CALTECH), Pasadena CA, United States. E-mail: hanlihao@caltech.edu

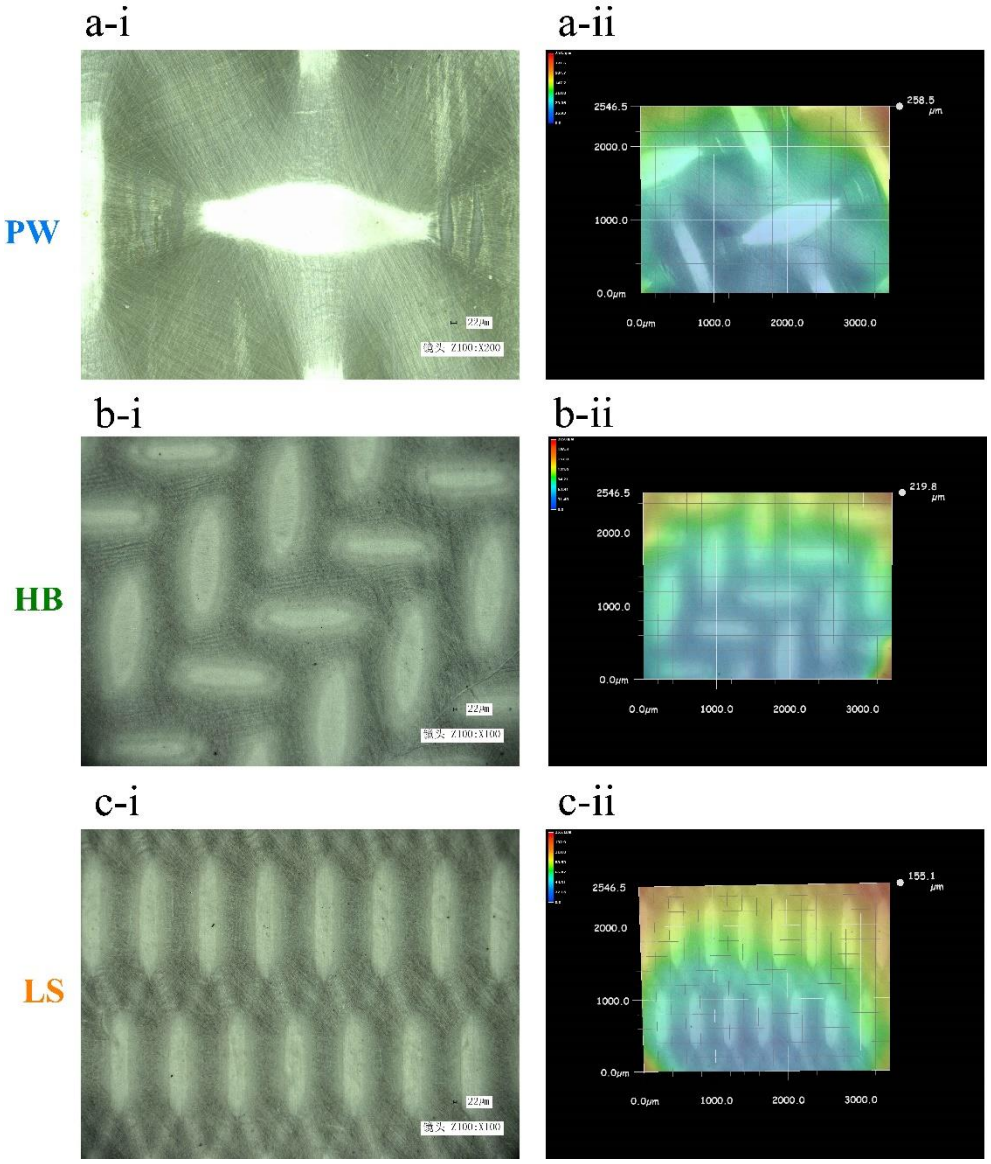

Figure S1. (i) Photomicrograph and (ii) The height distribution map for the surface of three patterned nanofibrous membranes. (a) PW NFs, (b) HB NFs and (c) LS NFs.

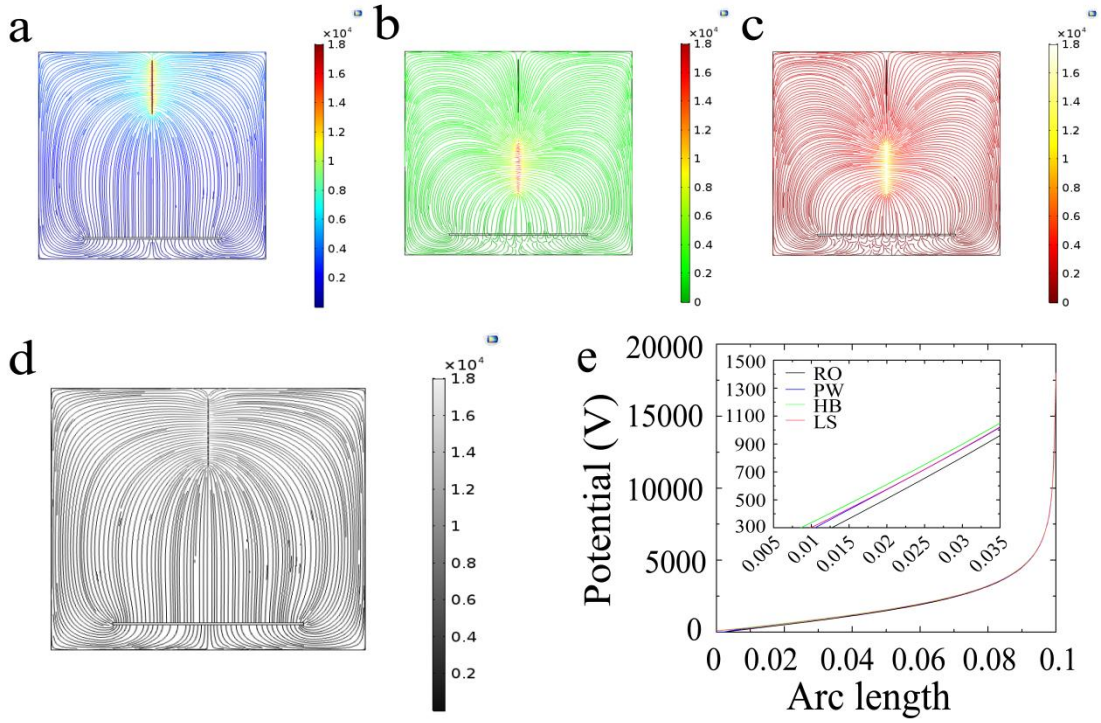

Figure S2. Electric field simulation for the formation process of patterned nanofibrous membranes: (a) PW NFs, (b) HB NFs, (c) LS NFs and (d) RO NFs, metal-needle-to-collector distance of 30 cm, and applied voltage of 19 kV. (e) The corresponding distribution of potential.

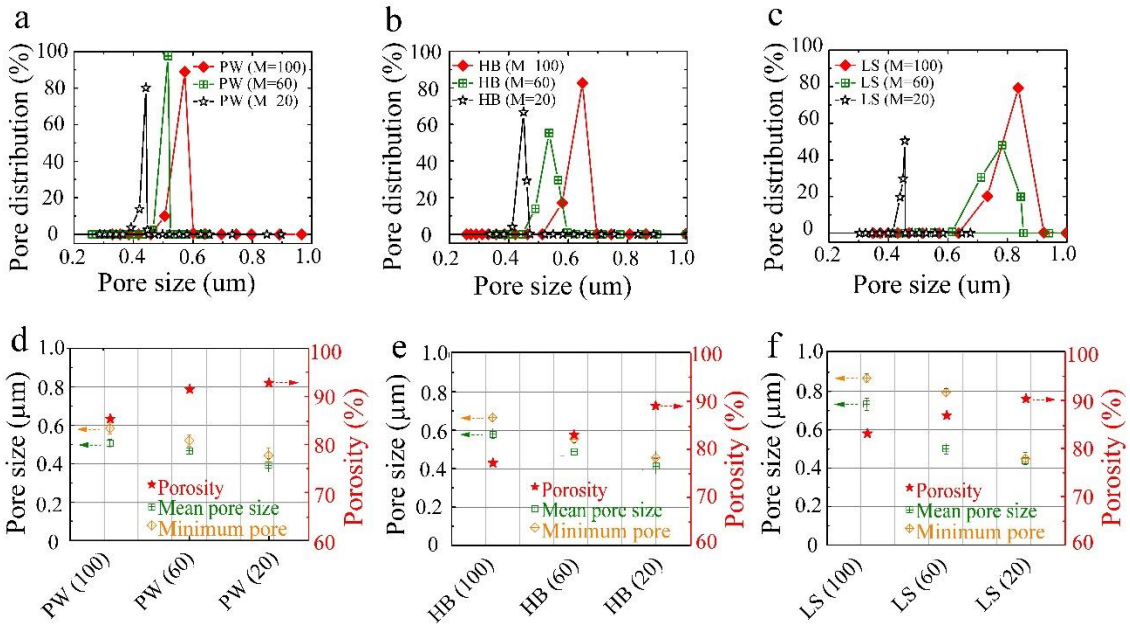

Figure S3. Pore size distribution analysis of the nanofibrous membranes: (a) PW NFs,

(b) HB NFs and (c) LS NFs. Mean pore size and minimum pore size of various nanofibrous membranes and its corresponding porosity: (d) PW NFs, (e) HB NFs and (f) LS NFs.

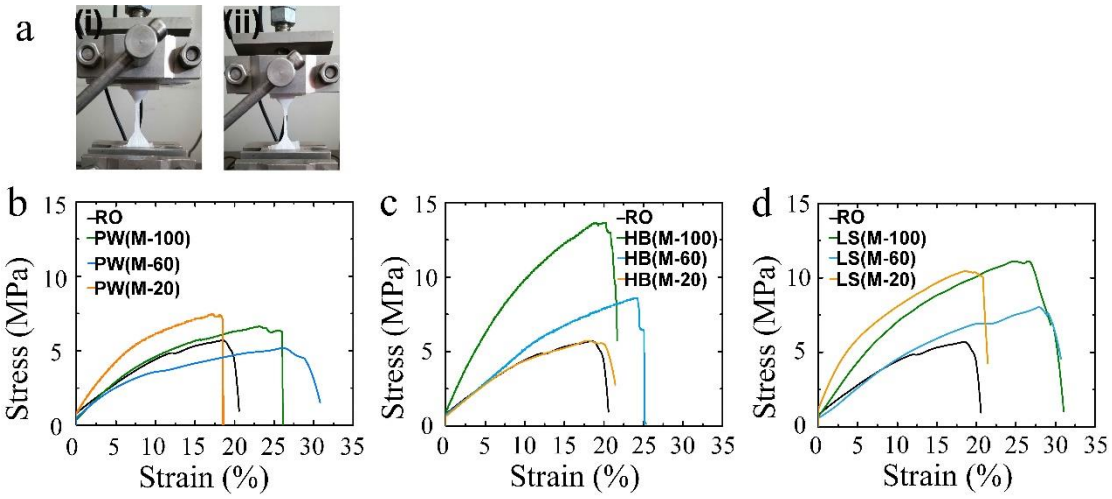

Figure S4. Tensile stress-strain curves of three patterned nanofibrous membranes with different mesh number.

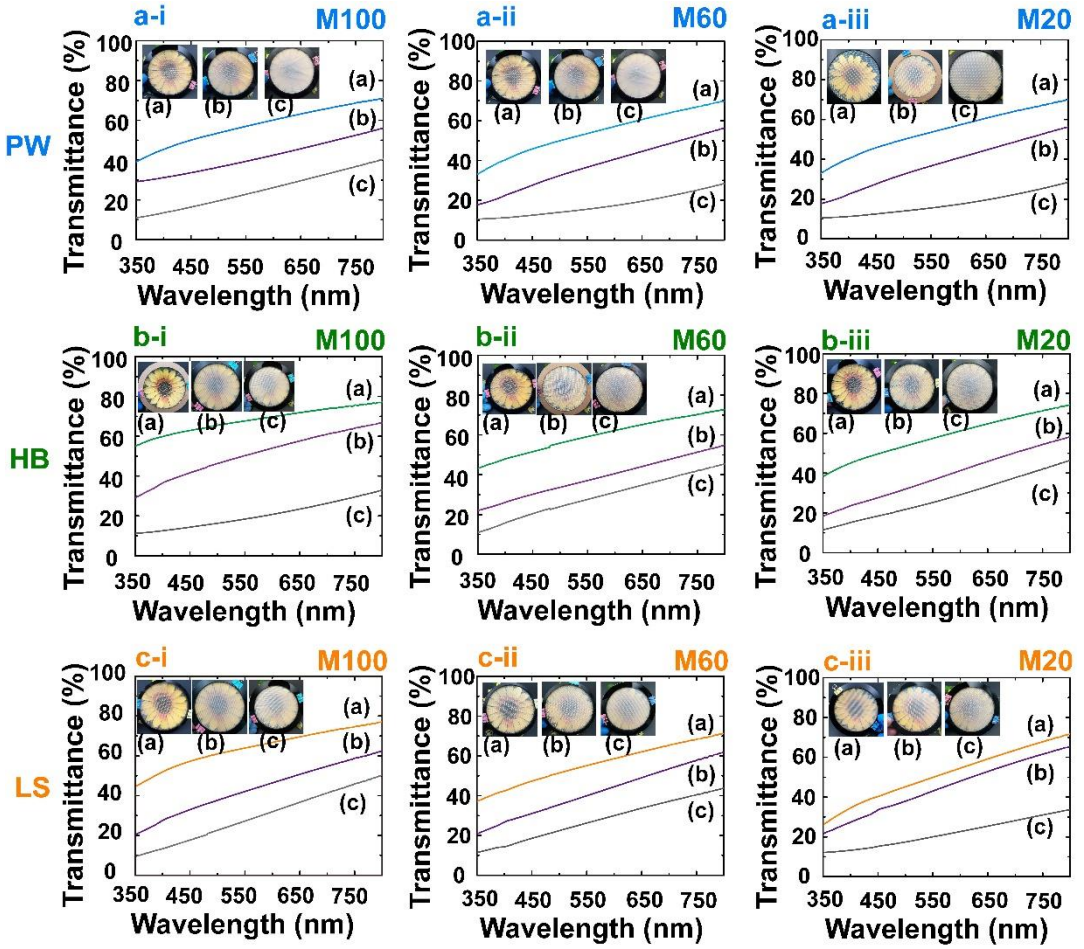

Figure S5. Light transmittance in the range of visible light wavelength of various patterned nanofibrous membranes with different thickness: (a) 4 μm; (b) 8 μm; (c) 16 μm.

Figure S6. Equipment of $PM_{2.5}$ purification efficiency measurement under simulated haze pollution.